Supplementary Information

Kinetics of isotropic to string-like phase switching in electrorheological fluids of nanocubes

Luca Tonti[1], Fabián A. García Daza[1], Alessandro Patti[1,2,*]

[1]*Department of Chemical Engineering, The University of Manchester, Manchester, M13 9PL, UK*
[2]*Department of Applied Physics, University of Granada, Fuente Nueva s/n, 18071 Granada, Spain*

[*]apatti@ugr.es

S1. Cluster criterion optimisation via density-based cluster analysis

Defining a criterion to recognize when cubes belong to chains is fundamental for the analysis of all the properties of chain-like structures. Due to the cylindrical symmetry of the chains and considering that their formation is driven only by dipolar interactions between the centers of mass of the particles, we characterized the connectivity between two particles i and j using their relative dipolar interaction energy: i and j are connected if $\beta u_{ij,dip} < \beta u_{max}$, where βu_{max} is the cluster parameter. Since $\beta u_{ij,dip}$ depends only on the relative distance between particles and the alignment of $\mathbf{r}_{ij}$ with the external field, we optimized βu_{max} from the analysis of the distribution of the first two smallest values of $\|\mathbf{r}_{ij}\|$ for each particle, named $\mathbf{r}_{ij,1}$ and $\mathbf{r}_{ij,2}$, extrapolated from an equilibrated string-like configuration of cubes, where $\mathbf{r}_{ij,1}$ and $\mathbf{r}_{ij,2}$ are decomposed in the direction parallel ($r_{ij,\parallel}$) and perpendicular ($r_{ij,\perp}$) to the orientation of the field. Most of the points of the data set are found in the proximity of the minimum of the interaction potential between two cubes, as expected for particles disposed one on top of the other and aligned with the external field (see Figure 1(a) for a plot of one sample data set).

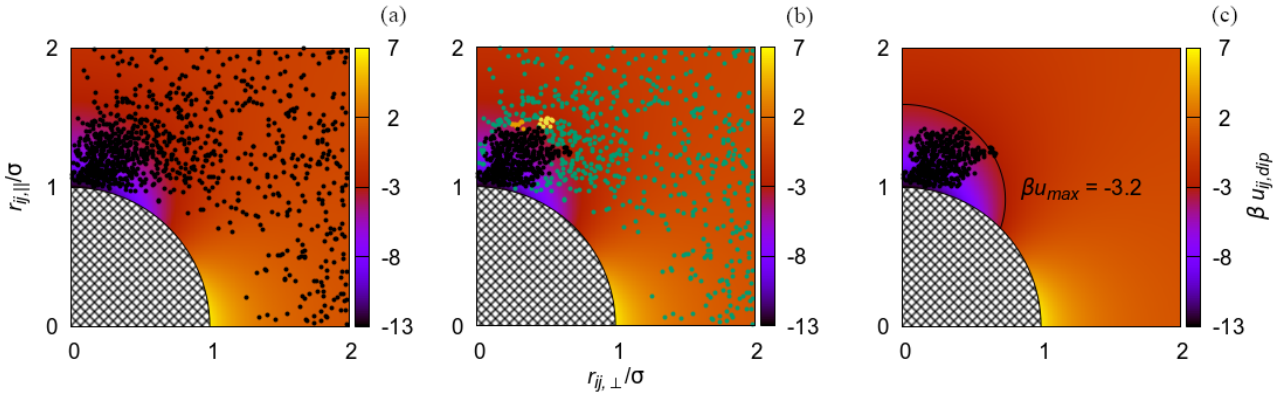

Figure 1: (a) Plot of the first and second closest particles j with respect to reference particle i, decomposed in the direction parallel and perpendicular to the external field, taken from a configuration of an equilibrated string-like phase of nanocubes. (b) Resulting clusters obtained from the application of DBSCAN algorithm to the points plotted in panel (a); points of the same color belong to a cluster according to DBSCAN. (c) Plot of the points of the cluster closest to the minimum of energy (black points), together with the contour line in which $\beta u_{ij,dip} = \beta u_{max}$. The background of each plot shows the value of the dipolar interaction energy $\beta u_{ij,dip}$ in color gradient, as a function of $r_{ij,\perp}$ and $r_{ij,\parallel}$. The patterned areas in black and white contain all the points for which $\|\mathbf{r}_{ij}\| < \sigma$, which are inaccessible due to hard core interactions between nanocubes.

In order to obtain an optimal value of βu_{max} for the analysis of the connectivity, we applied the DBSCAN clustering algorithm to the data set of the distances $\mathbf{r}_{ij}$. The DBSCAN algorithm analyses the local density of the data set, and assigns elements of the data set to a cluster if their density is higher than a threshold value [1]. It requires the definition of two parameters: *Eps*, which is the radius of the n-ball centered at element p; $MinPts$, which is the minimum number of elements q contained in the n-ball with radius *Eps* and center p. By

definition, the set of points q found in the n-ball centered at p with radius Eps is called "Eps-neighbourhood" of p, and the number of elements of this set is N_{Eps}:

$$N_{Eps}(p) = \#\{q \in D \,|\, dist(p,q) \leq Eps\} \tag{1}$$

where D is the data set. The algorithm starts from a random element p_0 and computes all the neighbouring elements q. If $N_{Eps} \geq MinPts$, a new cluster is found and is made of p_0 plus all the neighbouring elements q. At this point, DBSCAN reiterates the computation of the "Eps-neighbourhood" for each element q, as long as new neighbor elements are found. The set of all the "Eps-neighbourhoods" found starting from p_0 is a cluster. When the iteration stops, the algorithm restarts the analysis from a random element left of the data set, until the entire data set is covered. A schematic representation of one step of the algorithm is shown in Figure 2.

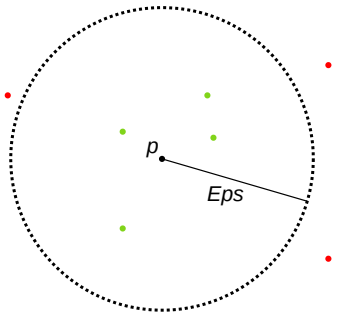

Figure 2: Representation of "Eps-neighbourhood" of p. All the points are elements of the data set. p is the initial element, Eps is the radius of the area in which we analyse the neighbourhood of p. Green points are elements that belong to the "Eps-neighbourhood" of p, while red points are outsiders. In one iteration, if the number of green points is $\geq MinPts$, then the green points plus p form a cluster, and the green points are chosen as new starting points p from which the cluster can be extended.

We performed density-based cluster analysis using the library DBSCAN available in R [2]. The algorithm was applied to 44 independent data sets, where each data set is extracted from uncorrelated configurations of an equilibrated chain-like phase of nanocubes. From each configuration, we computed the first ($\mathbf{r}_{ij,1}$) and second ($\mathbf{r}_{ij,2}$) closest distances between the centres of mass of two particles, with periodic boundary conditions, for all the particles of the configuration. Doubles of the distances $\mathbf{r}_{ij}$ were discarded. All the distances computed were saved as a 2D vector with components $(r_{ij,\parallel}, r_{ij,\perp})$. Since we were interested only in a portion of space were the energy reaches a minimum, we limited the data sets only to the points within the range $0 \leq r_{ij,\parallel}, , r_{ij,\perp} \leq 2$. An example of resulting data set extrapolated from a configuration is shown in Figure 1(a). We then applied DBSCAN to each data set independently, from which recovered only the points belonging to the cluster closest to the minimum of the energy. An example of application of the clustering algorithm to a data set is shown in Figure 1(b), where the cluster of interest is highlighted in black. We finally computed the maximum value of the energy $\beta u_{ij,dip}$ for the points of each recovered cluster: all the points of each cluster belong to a portion of the $(r_{ij,\perp}, r_{ij,\parallel})$ plot delimited by a contour line in which the energy is constant. We finally set the average of all contour energies of each data set as our threshold energy parameter $\beta u_{max} = \langle \beta u_{max} \rangle_{set} = -3.20$. Figure 1(c) shows the the elements of the desired cluster extrapolated with DBSCAN, contained in the area delimited by the countour line in which $\beta u_{ij,dip} = \beta u_{max}$.

S2. Renormalisation of the uniaxial order parameter for particles with cubic symmetry

The most favoured configuration of two polarised nanocubes is for their two centers of mass to be relatively aligned with the external field and to be as close as possible, thus having one of their faces in contact with each other, and with these faces orthogonal to the orientation of the field $\hat{\mathbf{E}}$. For this reason, the orientational order of the cubic particles with respect to the external field, which can be evaluated with the uniaxial order parameter $U = \langle P_2(\hat{\mathbf{E}} \cdot \hat{\mathbf{e}}_i)\rangle$ (P_2 is the second Legendre polynomial), can indirectly give information on the formation of chain-like structures. However, due to the geometry of cubes, each of the three axes of orientation $\hat{\mathbf{e}}_1$, $\hat{\mathbf{e}}_2$, $\hat{\mathbf{e}}_3$ of every particle can be equivalently aligned with $\hat{\mathbf{E}}$ when they organise in chains. To overcome this issue, Batten *et al.* [3], in their work on the investigation of the phase behaviour of colloidal superballs, suggested to "relabel" particles axes of orientation according to their best alignment with the reference axes, hence for a reference axis $\hat{\mathbf{n}}$ they computed $\langle P_2(\max((|\hat{\mathbf{n}} \cdot e_k|), k = 1, 2, 3)\rangle$. Since in our case the director along which particles should be aligned is known and it is the orientation of the external field $\hat{\mathbf{E}}$, we computed the average of the alignment between $\hat{\mathbf{n}}$ and the most aligned axis $\hat{\mathbf{e}}_k$ of each cube, for $\hat{\mathbf{n}} = \hat{\mathbf{E}}$

$$\left\langle \max\left((\hat{\mathbf{n}} \cdot \hat{\mathbf{e}}_k)^2\right), i = \{1, 2, 3\} \right\rangle \tag{2}$$

Here we report the formal proof developed to normalize the order parameter in Eq. 2.

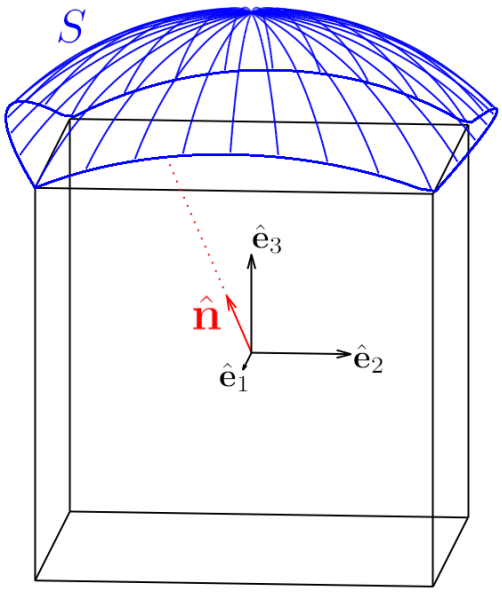

Figure 3: Cubic particle (black lines) topped with a portion of a sphere with surface S (in blue). $\hat{\mathbf{e}}_1$, $\hat{\mathbf{e}}_2$, $\hat{\mathbf{e}}_3$ are the three axes of orientation of the cube, originated from the center of mass. Red arrow shows one possible direction of the director $\hat{\mathbf{n}}$ and the red dot line is its extension up to surface S. S is the area in which integrate $(\hat{\mathbf{n}} \cdot \hat{\mathbf{e}}_3)^2$ for normalisation of the order parameter, where $\hat{\mathbf{e}}_3$ is here the most aligned axis with $\hat{\mathbf{n}}$.

Figure 3 shows one cube, with its axes of orientation, here tkaed as reference axes, and the director $\hat{\mathbf{n}}$ with one possible orientation with respect to $\hat{\mathbf{e}}_1$, $\hat{\mathbf{e}}_2$, and $\hat{\mathbf{e}}_3$. The prolongation of $\hat{\mathbf{n}}$ intersects always the surface of the cube. Due to the symmetry of the cube, for each possible direction of $\hat{\mathbf{n}}$, the most aligned axis of orientation $\hat{\mathbf{e}}_k$ with $\hat{\mathbf{n}}$ will always be the one orthogonal to the face whom the prolongation of $\hat{\mathbf{n}}$ intersects. This means that Eq. 2 can be normalised integrating only over the possible orientations of $\hat{\mathbf{n}}$ with respect to one of the faces of the cube: this normalisation corresponds to integrate $(\hat{\mathbf{n}} \cdot \hat{\mathbf{e}}_k)^2$ over one sixth of the surface of a unit sphere, which is schematically represented in Figure 3 with blue lines, and all the angles between $\hat{\mathbf{n}}$ and one $\hat{\mathbf{e}}_k$, for which the extension of $\hat{\mathbf{n}}$ intersects the edges of one face of the cube, are boundaries of the integral. We can define $\hat{\mathbf{n}}$ in spherical coordinates as a function of two angles θ and ϕ with respect to the axes of orientation of the cube and recover the following definitions, according to the geometric representation in Figure 4 and

assuming that the cube has unit length

$$\widehat{AO'H} = \phi$$
$$\widehat{HOO'} = \theta$$
$$\widehat{AO'B} = \frac{\pi}{4}$$
$$\widehat{HBO} = \widehat{BO'O} = \widehat{ABO'} = \frac{\pi}{2}$$
$$\overline{OH} = x$$
$$\overline{HB} = y$$
$$\overline{AO'} = \overline{OB} = \frac{1}{\sqrt{2}}$$
$$\overline{O'B} = \overline{OO'} = \frac{1}{2}$$

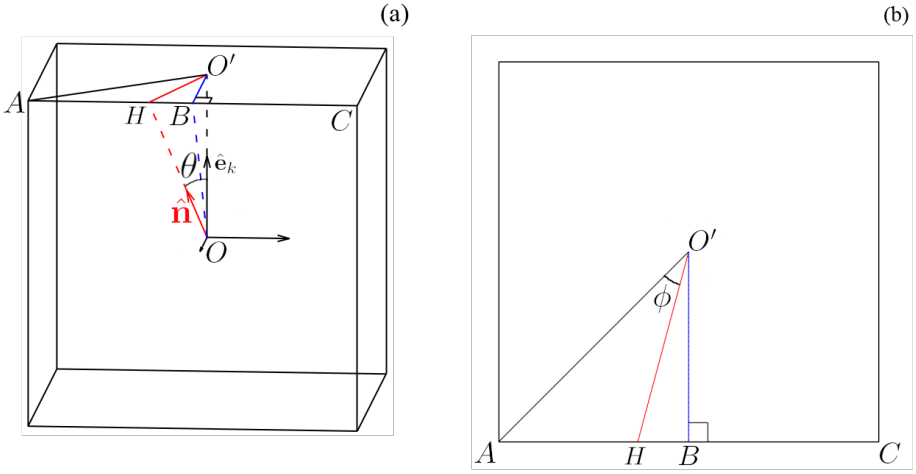

Figure 4: Geometric representation of the cube with the director $\hat{\mathbf{n}}$. Panel (a, left) shows the cube and all the projections in 3D; panel (b, right) shows the view from the top face of the cube. O is the center of mass of the cube. O' is the projection of O on the top face of the cube. A and C are two of the vertices of the cube. $\overline{AC}$ is one edge of the top face of the cube. B is the midpoint of $\overline{AC}$. Dashed blue line connects the origin O with the midpoint B, and straight blue line is the projection of $\overline{OB}$ on the top face of the cube. Both $\overline{OB}$ and $\overline{AO'}$ are half of the diagonal of one face of the cube. Both $\overline{O'B}$ and $\overline{OO'}$ are half of the length of one edge of the cube. Red arrow and dashed red line are, respectively, the unit vector $\hat{\mathbf{n}}$ and its extension $\overline{OH}$ to the edge $\overline{AC}$; the extension of $\hat{\mathbf{n}}$ intersect $\overline{AC}$ at H. Straight red line is the projection of $\overline{OH}$ on the top face of the cube. θ is the angle between $\hat{\mathbf{n}}$ and $\hat{\mathbf{e}}_k$. ϕ is the angle between the projection $\overline{AO'}$ and the projection $\overline{O'H}$.

Thanks to geometry, we can recover the link between θ and ϕ for the case when $\hat{\mathbf{n}}$ intersect the edges of one of the faces of the cube. If $0 \leq \phi < \pi/4$, the following equations hold

$$\cos(\theta) = \frac{\overline{OO'}}{\overline{OH}} = \frac{1}{2x}$$
$$x = \overline{OH} = \sqrt{\overline{OB}^2 + \overline{HB}^2} = \sqrt{\left(\frac{1}{\sqrt{2}}\right)^2 + y^2}$$
$$y = \overline{HB} = \overline{O'B}\tan\left(\widehat{HO'B}\right) = \frac{\tan\left(\frac{\pi}{4} - \phi\right)}{2}$$
$$\cos(\theta) = \frac{1}{\sqrt{2 + \tan^2\left(\frac{\pi}{4} - \phi\right)}} = f^{(+)}(\phi) \tag{3}$$

For $\pi/4 \leq \phi < \pi/2$, Eq. 3 holds since $\tan^2(x)$ is an even function. For $\pi/2 \leq \phi < 3\pi/4$, we obtain

$$y = \frac{\tan\left(\phi - \frac{\pi}{4} - \frac{\pi}{2}\right)}{2} = \frac{-\cot\left(\phi - \frac{\pi}{4}\right)}{2}$$

$$\cos(\theta) = \frac{1}{\sqrt{2 + \cot^2\left(\frac{\pi}{4} - \phi\right)}} = f^{(-)}(\phi) \tag{4}$$

The validity of Eq. 4 is extended to $3\pi/4 \leq \phi < \pi$ for the same reason as Eq. 3. Since both Eq. 3 and 4 are periodic to π, we can define the link between θ and ϕ along the border of one face of the cube as follows

$$\cos(\theta) = \begin{cases} f^{(+)}(\phi) & if \quad 0 \leq \phi < \frac{\pi}{2} \cup \pi \leq \phi < \frac{3\pi}{2} \\ f^{(-)}(\phi) & if \quad \frac{\pi}{2} \leq \phi < \pi \cup \frac{3\pi}{2} \leq \phi < 2\pi \end{cases} \tag{5}$$

The average value of the order parameter for a uniform distribution of $\hat{\mathbf{n}}$ can be estimated according to the following integral

$$\left\langle \max\left((\hat{\mathbf{n}} \cdot \hat{\mathbf{e}}_k)^2\right)\right\rangle = \frac{\int\int_S \cos^2(\theta)\sin(\theta)d\theta d\phi}{\int\int_S \sin(\theta)d\theta d\phi} \tag{6}$$

where the limits of S depend on Eq. 5. We first compute the integral in the denominator of Eq. 6

$$\int\int_S \sin(\theta)d\theta d\phi = \int_0^{\arccos(f^{(+)}(\phi))}\int_0^{\pi/2} \sin(\theta)d\theta d\phi + \int_0^{\arccos(f^{(-)}(\phi))}\int_{\pi/2}^{\pi} \sin(\theta)d\theta d\phi +$$
$$+ \int_0^{\arccos(f^{(+)}(\phi))}\int_{\pi}^{3\pi/2} \sin(\theta)d\theta d\phi + \int_0^{\arccos(f^{(-)}(\phi))}\int_{3\pi/2}^{2\pi} \sin(\theta)d\theta d\phi$$

We substitute $\int \sin(\theta)d\theta = -\cos(\theta)$, $\cos(0) = 1$ and $\cos(\arccos(f(\phi))) = f(\phi)$ in the integral

$$\int\int_S \sin(\theta)d\theta d\phi = \int_0^{\pi/2}\left[1 - f^{(+)}(\phi)\right]d\phi + \int_{\pi/2}^{\pi}\left[1 - f^{(-)}(\phi)\right]d\phi + \int_{\pi}^{3\pi/2}\left[1 - f^{(+)}(\phi)\right]d\phi + \int_{3\pi/2}^{2\pi}\left[1 - f^{(-)}(\phi)\right]d\phi \tag{7}$$

Since both $f^{(+)}$ and $f^{(-)}$ are periodic with period π and $\tan^2(x) = \cot^2(x - \pi/2)$, the following equalities hold

$$\int_0^{\pi/2} f^{(+)}(\phi)d\phi = \int_{\pi/2}^{\pi} f^{(-)}(\phi)d\phi = \int_{\pi}^{3\pi/2} f^{(+)}(\phi)d\phi = \int_{3\pi/2}^{2\pi} f^{(-)}(\phi)d\phi \tag{8}$$

Hence, integral in Eq. 7 simplifies

$$\int\int_S \sin(\theta)d\theta d\phi = 2\pi - 4\int_0^{\pi/2} f^{(+)}d\phi$$

It can be proved that

$$\int_0^{\pi/2} f^{(+)}d\phi = \int_{-\pi/4}^{\pi/4} \frac{\cos(\phi)}{\sqrt{2 - \sin^2(\phi)}}d\phi = \frac{\pi}{3}$$

The solution of the integral is

$$\int\int_S \sin(\theta)d\theta d\phi = 2\pi - 4\frac{\pi}{3} = \frac{2\pi}{3} \tag{9}$$

This is what we should expect for this geometry: the surface we integrated over is exactly one sixth of the surface of a unit sphere (since we have integrated the surface of a unit sphere only for those angles of θ and ϕ for which the intersection of the prolongation of $\hat{\mathbf{n}}$ with the surface of the cube is contained in one face of the cube).

In order to solve the integral in the numerator of Eq. 6, we use the equality $\int \cos^2(\theta)\sin(\theta)dx = -\cos^3(\theta)/3$ and we obtain an equation similar to Eq. 7, with $[f^{(+)}]^3$ instead of $f^{(+)}$, and $[f^{(-)}]^3$ instead of $f^{(-)}$. Since the equalities in Eq. 8 hold also in this case, the desired integral can be simplified as follows

$$\int\int_S \cos^2(\theta)\sin(\theta)d\theta d\phi = \frac{2\pi}{3} - \frac{4}{3}\int_0^{\pi/2}\left[f^{(+)}(\phi)\right]^3 d\phi$$

It can be proved that

$$\int_0^{\pi/2} \Big[f^{(+)}(\phi)\Big]^3 d\phi = \int_{-\pi/4}^{\pi/4} \frac{1-\sin^2(\phi)}{\big[2-\sin^2(\phi)\big]^{3/2}} \cos(\phi) d\phi = \frac{\pi}{3} - \frac{1}{\sqrt{3}} \tag{10}$$

In conclusion, the integral in the numerator of Eq. 6 is

$$\int\int_S \cos^2(\theta)\sin(\theta) d\theta d\phi = \frac{2\pi}{3} - \frac{4}{3}\left(\frac{\pi}{3} - \frac{1}{\sqrt{3}}\right) = \frac{2\pi + 4\sqrt{3}}{9} \tag{11}$$

Finally, we substitute Eq. 9 and Eq. 11 into Eq.6 to recover the expected value of $\max((\hat{\mathbf{n}}\cdot\hat{\mathbf{e}}_k)^2)$ for a uniform distribution of orientations of $\hat{\mathbf{n}}$

$$\Big\langle \max\Big((\hat{\mathbf{n}}\cdot\hat{\mathbf{e}}_k)^2\Big)\Big\rangle = \frac{\frac{2\pi+4\sqrt{3}}{9}}{\frac{2\pi}{3}} = \frac{\pi+2\sqrt{3}}{3\pi} \tag{12}$$

As a proof that this value is indeed correct, we remark that Batten *et al.* noticed that, for an isotropic phase of superballs, $\langle P_2(\max(\hat{\mathbf{n}}\cdot\hat{\mathbf{e}}_k))\rangle \approx 0.55$, which is exactly what we obtain:

$$\Big\langle P_2\Big(\max\big(|\hat{\mathbf{n}}\cdot\hat{\mathbf{e}}_k|\big)\Big)\Big\rangle = \frac{1}{2}\Big\langle 3\max\Big((\hat{\mathbf{n}}\cdot\hat{\mathbf{e}}_k)^2\Big) - 1\Big\rangle = \frac{1}{2}\left(3\frac{\pi+2\sqrt{3}}{3\pi} - 1\right) = \frac{\sqrt{3}}{\pi} \approx 0.55$$

Normalising $\max((\hat{\mathbf{n}}\cdot\hat{\mathbf{e}}_k)^2)$ with the result in Eq. 12 and imposing that the parameter goes to 1 when $\max((\hat{\mathbf{n}}\cdot\hat{\mathbf{e}}_k)^2) = 1$, *i.e.* when the cube is perfectly aligned with $\hat{\mathbf{n}}$, we can finally obtain a renormalised uniaxial order parameter for particles with cubic symmetry

$$S = \frac{1}{N}\sum_{i=1}^{N} S_i = \frac{1}{N}\sum_{i=1}^{N} \frac{\pi\Big(3\max\big((\hat{\mathbf{n}}\cdot\hat{\mathbf{e}}_{k,i})^2, k=1,2,3\big) - 1\Big) - 2\sqrt{3}}{2\pi - 2\sqrt{3}} \tag{13}$$

S3. Mean square displacement of a spherical tracer immersed in a bath of nanocubes

Figures 5 and 6 depict the mean square displacement (MSD) of a spherical tracer immersed in a bath of nanocubes with side σ at packing fractions $\eta = 0.02$ and $\eta = 0.2$, respectively. The MSD is estimated when the external field is on and off. The MSD of the tracer particle can be defined from the tracer's position $\mathbf{r}_d(t)$ at time t as follows

$$\langle \Delta \mathbf{r}_d^2(t) \rangle = \langle (\mathbf{r}_d^2(t) - \mathbf{r}_d^2(0))^2 \rangle \tag{14}$$

where the brackets refer to the averages over independent trajectories, and d is the dimensionality of the displacements of the tracer. While the value $d = 3$ indicates the total MSD of the tracer particle, $d = 2$, and 1 refer, respectively, to the MSDs perpendicular and parallel to the external field. To calculate the MSDs we have run 1000 uncorrelated trajectories to simulate the motion of the tracer and bath particles.

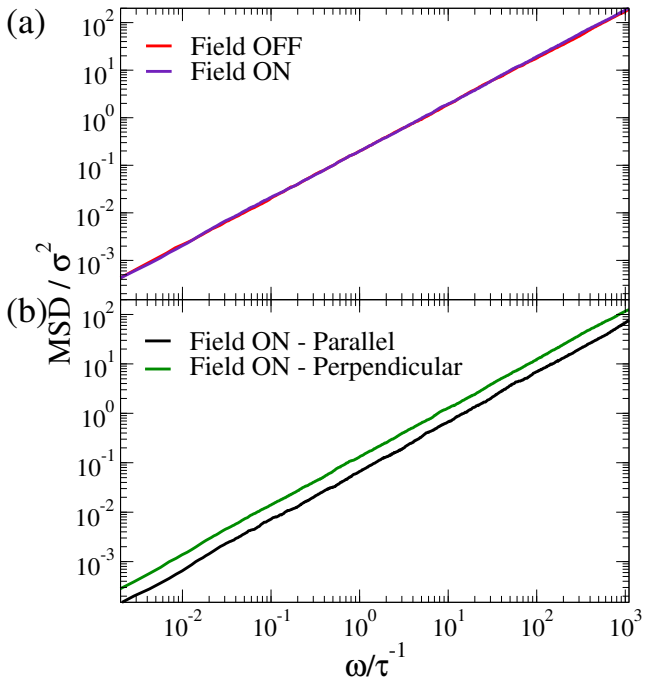

Figure 5: (Color on-line) Mean square displacement of a spherical tracer of size 3σ diffusing across a bath of nanocubes of side σ at a packing fraction $\eta = 0.02$. Top panel: MSD calculated in the three spatial coordinates when the external field is on (blue line) and off (red line). Bottom panel: MSD parallel (black line) and perpendicular (green line) to the external field, when the field is on.

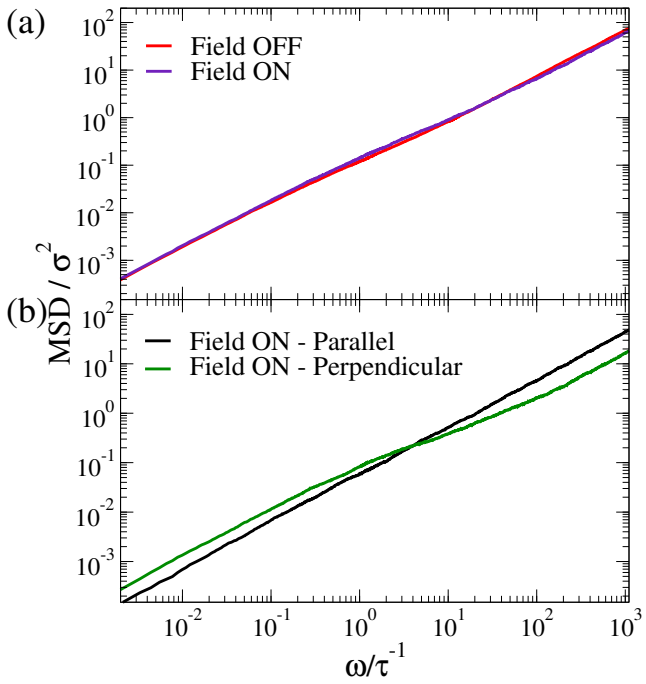

Figure 6: (Color on-line) Mean square displacement of a spherical tracer of size 3σ diffusing across a bath of nanocubes of side σ at a packing fraction $\eta = 0.2$. Top panel: MSD calculated in the three spatial coordinates when the external field is on (blue line) and off (red line). Bottom panel: MSD parallel (black line) and perpendicular (green line) to the external field, when the field is on.

S4. Benchmarking between the Fourier and compliance-based methods to calculate the elastic and viscous moduli of a bath of nanocubes

The compliance methods [4, 5] intend to transform the time dependent compliance ($J(t)$) of the material to estimate its corresponding complex modulus ($G^*(\omega)$) in the frequency domain. The compliance can be expressed as

$$J(t) = \left(\frac{\pi a_{sph}}{k_{\mathrm{B}}T}\right)\langle\Delta r^2(t)\rangle, \tag{15}$$

where a_{sph} indicates the radius of the tracer, k_{B} the Boltzmann's constant, T the temperature, and $\langle\Delta r^2(t)\rangle$ the tracer's mean square displacement (MSD). According to Evans *et al.* [4], $J(t)$ can be related to $G^*(\omega)$ by

$$\frac{i\omega}{G^*(\omega)} = \left(1 - e^{-1\omega t_1}\right)\frac{J(t_1)}{t_1} + 6De^{-i\omega t_{N_t}} + \sum_{k=2}^{N_t}\frac{J_k - J_{k-1}}{t_k - t_{k-1}}\left(e^{-i\omega t_{k-1}} - e^{-i\omega t_k}\right), \tag{16}$$

where N_t denotes the number of points within the time window where the MSD was computed, D is linked to the inverse of the system's viscosity, and J_k refers to $J(t)$ at time t_k. The solution of Eq. 16 results in the viscous ($G''(\omega)$) and elastic ($G'(\omega)$) moduli since $G^*(\omega) = G'(\omega) + iG''(\omega)$.
The comparison between $G''(\omega)$ and $G'(\omega)$ calculated by the Fourier approach by Mason [6] and the compliance method proposed by Evans *et al.* [4] is presented in Fig. 7. In both cases, the MSD of a spherical tracer with size 3σ diffusing in a bath of nanocubes is calculated when the external field is on and off.

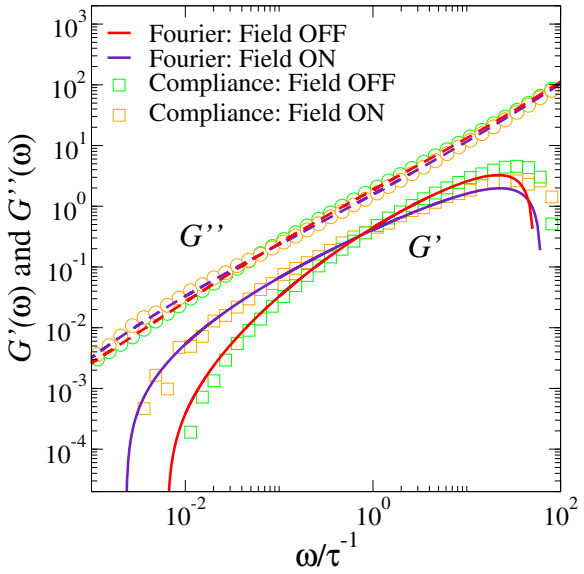

Figure 7: (Color on-line) Viscous $G''(\omega)$ (empty circles, dashed lines) and elastic $G'(\omega)$ (empty squares, solid lines) moduli obtained by the Fourier approach [6] (lines) and the compliance-based method [4] (symbols) for an bath of nanocubes containing a spherical tracer of size 3σ. Two scenarios were explored: when the external field is on (orange symbols, blue curves) and off (green symbols, red curves).

References

[1] Ester, M., Kriegel, H. P., Sander, J. & Xu, X. A Density-Based Algorithm for Discovering Clusters in Large Spatial Databases with Noise. In *Proceedings of the Second International Conference on Knowledge Discovery and Data Mining*, 226 (1996).

[2] Hahsler, M., Piekenbrock, M. & Doran, D. dbscan: Fast Density-Based Clustering with R. *Journal of Statistical Software* **91**, 1 (2019).

[3] Batten, R., Stillinger, F. H. & Torquato, S. Phase behavior of colloidal superballs: Shape interpolation from spheres to cubes. *Phys. Rev. E* **81**, 061105 (2010).

[4] Evans, R. M. L., Tassieri, M., Auhl, D. & Waigh, T. A. Direct conversion of rheological compliance measurements into storage and loss moduli. *Phys. Rev. E* **80**, 012501 (2009).

[5] Nishi, K., Kilfoil, M. L., Schmidt, C. F. & MacKintosh, F. C. A symmetrical method to obtain shear moduli from microrheology. *Soft Matter* **14**, 3716 (2018).

[6] Mason, T. G. Estimating the viscoelastic moduli of complex fluids using the generalized Stokes–Einstein equation. *Rheol. Acta* **39**, 371 (2000).